Progress In Electromagnetics Research Letters, Vol. 107, 93–101, 2022

Broadband Proximity Coupled Millimeter-Wave Microstrip Array Antenna for Automotive Radar Applications

Shuo Wang[1], Dan Zhang[1, *], Zhendong Ding[2], Huiwen Chen[1], and Shenxiang Yang[1]

Abstract—In this letter, a broadband proximity coupled millimeter-wave microstrip array antenna is presented for automotive radar applications. The antenna array consists of a microstrip line and a series of trapezoidal radiating elements that are periodically arranged on both sides of the microstrip line, at intervals of about half the guided-wavelength. The introduction of the trapezoidal radiating patch enhances the excitation coupling while suppressing out-of-band frequencies, and it has a wider impedance bandwidth than the rectangular patch. In the design of proposed antenna, the normalized resistance of the trapezoidal radiating element is controlled by adjusting the gap with the microstrip line, so that a low-sidelobe level (SLL) can be achieved. Taking the 77–81 GHz frequency band allocated to automotive radar applications as an example, a 1×16 linear array is designed and fabricated. The measured SLL is better than -20 dB. The measured gain of 1×16 array is higher than 15 dBi over the operating frequency range of 77–81 GHz. The 1×16 linear array can achieve an impedance bandwidth of 7.6% (75.6–81.6 GHz).

1. INTRODUCTION

With the continuous improvement of the requirements for safe driving, millimeter-wave array antennas have been widely studied and applied in automotive radar [1]. Because microstrip patch antenna has the advantages of low profile, low manufacturing cost, and easy installation, it is very competitive in application value in the millimeter wave band [2]. Microstrip patch antennas have been widely used in automotive anti-collision radars, especially in the 77 GHz frequency band, but due to the feed loss caused by microstrip line transmission, it will be challenging to design microstrip antennas with low SLL and wide bandwidth [3]. Therefore, it is urgent to design a millimeter-wave microstrip antenna with good performance and a simple and compact structure.

The commonly used direct-feed structure of microstrip array can be divided into parallel feed [4–7] and series feed [8–11]. Generally, it is relatively easier to obtain wide bandwidth and stable gain with parallel-fed arrays [4–7]. However, parallel-fed arrays usually have additional losses because of the bulky feed network. Conversely, series-fed microstrip array antennas usually have a simpler feed network and more compact structure; however, the arrays tend to have a narrower impedance bandwidth. For example, the series-fed microstrip arrays proposed in [8–11] have impedance bandwidths of 2.8%, 3.3%, 3.9%, and 1.24%, respectively.

Therefore, an indirect proximity coupled structure is introduced, so that the array antenna has a wider impedance bandwidth (5–10%) [12–14]. The main characteristic of proximity coupling is that its coupling mechanism is capacitive in nature, while direct-feed is inductive. The difference in the coupling mechanism enables the proximity coupled feed method to obtain a wider bandwidth, and the length and width of the feedline are adjusted for impedance matching.

Received 6 September 2022, Accepted 19 October 2022, Scheduled 28 October 2022

* Corresponding author: Dan Zhang (zhangdan@njfu.edu.cn).

[1] College of Information Science and Technology, Nanjing Forestry University, Nanjing 210037, China. [2] School of Electronic and Optical Engineering, Nanjing University of Science and Technology, Nanjing 210094, China.

In this letter, in order to take into account the broadband characteristics of the indirect proximity coupled structure and the easy formation of a linear array by the series feed structure, a novel broadband proximity coupled millimeter-wave microstrip array antenna is proposed for automotive radar applications. Trapezoidal radiating elements are periodically arranged on both sides of the microstrip line to form indirect proximity coupling, so that the antenna has a wider impedance bandwidth. By adjusting the gap between the radiating element and microstrip line, amplitude taper distribution is achieved. The microstrip 16-element linear array is designed and fabricated. The characteristics of broadband and SLL are in good agreement with the simulation results.

2. ANTENNA DESIGN AND ANALYSIS

This section details the design principles and analysis of millimeter-wave microstrip array antennas. By adjusting the gap between the radiating elements and microstrip line, the amplitude of the proposed proximity coupled millimeter-wave microstrip array antenna satisfies the Taylor-distribution and exhibits a -20 dB low-SLL. The entire design and analysis use a full-wave electromagnetic solution to the HFSS15.0 and optimize the antenna simulation results.

2.1. Antenna Configuration

Figure 1 shows the structure of the proposed broadband proximity coupled mmWave microstrip array antenna. The antenna is composed of a microstrip line with width W_f and a trapezoidal radiating element with upper bottom a, lower bottom b, and height h. An RO3003 substrate (relative dielectric constant $\varepsilon_r = 3.0$, loss tangent $\tan\delta = 0.0013$) is used in this paper, and its thickness is 0.127 mm. The antenna structure is printed on the top layer of the substrate, and the bottom layer is ground. Each trapezoidal radiating element appears alternately on both sides of the microstrip line, and the gap between the radiating element and microstrip line is d_n. The microstrip line terminal is open, and the working mode of the antenna is standing-wave. The radiating element is excited by the microstrip line through proximity electromagnetic coupling. The interval between the elements is half the guided-wavelength ($\lambda_g/2$), which makes each element excited in phase.

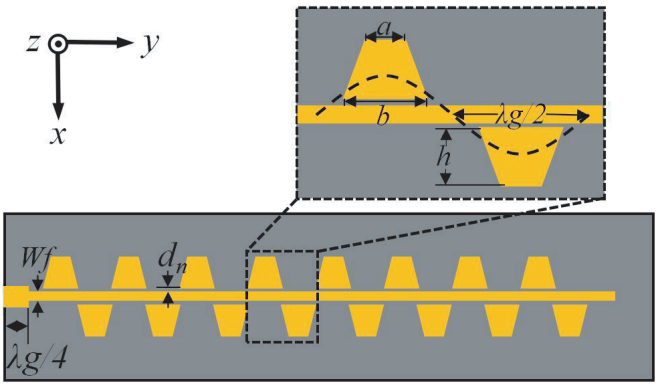

Figure 1. Structure of the proposed broadband proximity coupled millimeter-wave microstrip array antenna.

2.2. Principle Analysis of Linear Array Antenna

First, the antenna unit is composed of an open-circuit microstrip line excited by direct feeding and a coupling parasitic patch, as shown in Fig. 2(a). Assuming that the trapezoidal parasitic unit is 1, and the direct excitation microstrip line unit is 2, the circuit relationship between the units is as follows:

$$0 = I_1 Z_{11} + I_2 Z_{12} \tag{1}$$

$$V_2 = I_1 Z_{21} + I_2 Z_{22} \tag{2}$$

Thus

$$\frac{I_1}{I_2} = -\frac{Z_{12}}{Z_{11}} = me^{j\phi}$$
$$\text{where} \quad m = \sqrt{\frac{R_{12}^2 + X_{12}^2}{R_{11}^2 + X_{11}^2}} \tag{3}$$
$$\phi = \pi + \text{arctg}\frac{X_{12}}{R_{12}} - \text{arctg}\frac{X_{11}}{R_{11}}$$

Among them, $Z_{12} = R_{12} + jX_{12}$ is the mutual impedance between the trapezoidal parasitic unit 1 and direct excitation microstrip line unit 2, and $Z_{11} = R_{11} + jX_{11}$ is the self-impedance of the parasitic unit. It can be seen from Equation (3) that the amplitude and phase of the induced current on the parasitic unit depend on the self-impedance of the parasitic unit itself and its relationship with mutual impedance between stimulated units.

As shown in Fig. 2(b), the center of the trapezoidal patch is located at the maximum current, and the magnetic field distribution reaches the maximum, forming magnetic coupling, corresponding to the inductance ($L2$) on the equivalent circuit. The proximity coupling of the gap is equivalent to the series capacitance ($C1$). Therefore, the value of mutual impedance Z_{12} is determined by $C1$ and $L2$. By adjusting the size of the parasitic unit and the gap between the parasitic unit and excitation unit, the mutual impedance can be changed, thus changing the input impedance of the antenna to expand the antenna bandwidth. Because the distance from the center of the unit designed to the terminal of the open-circuit microstrip line is $3\lambda_g/4$, the impedance of the corresponding direct excitation microstrip unit is short circuit, which can be equivalent to series resonance ($R1L1C2$).

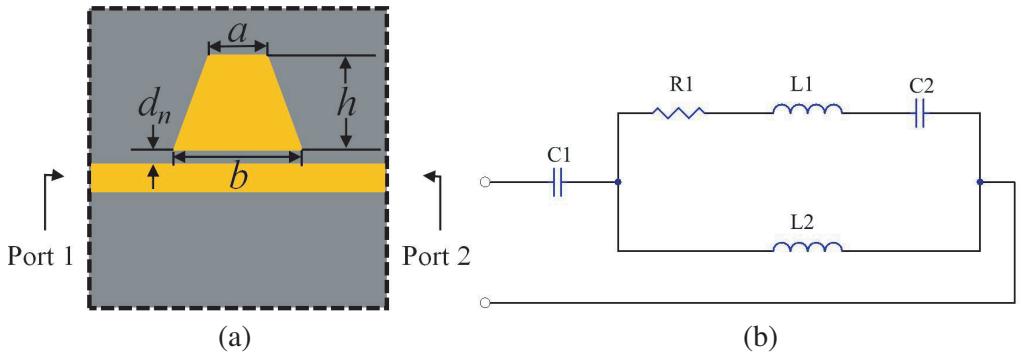

Figure 2. Unit analysis. (a) Trapezoidal radiating element. (b) Equivalent circuit.

Secondly, the simulated S_{11} of the proposed linear array with different lower bottom b widths of the trapezoidal radiating elements parameters are studied in Fig. 3. It can be seen that as b increases, both resonant modes are shifted downward, providing a wider impedance bandwidth. The currents of different frequencies pass through the open-circuit microstrip line, and the corresponding positions of the anti-nodes are different. At the center frequency, the center of the patch corresponds to the maximum position of the current. When the array is formed, the array elements work in the same phase, and the radiation field in the side-fire direction is enhanced by superposition; while for the out-of-band frequency, the coupling current generated on the patch is out of phase, the current between the patches is even out of phase at a specific frequency, and the radiation is suppressed. So, it can be seen from the subgraph of Fig. 1 that the trapezoidal patch at the central position relative to the rectangular patch not only is conducive to phase superposition, but also can suppress the out of band frequency, which has certain filtering characteristics.

Then, since the radiating element can be equivalent to series impedance, the two-port network method is used to analyze its impedance characteristics. Using the technology of setting Waveport, adjust the reference plane when calculating the S-parameter, and remove the influence of the feed line.

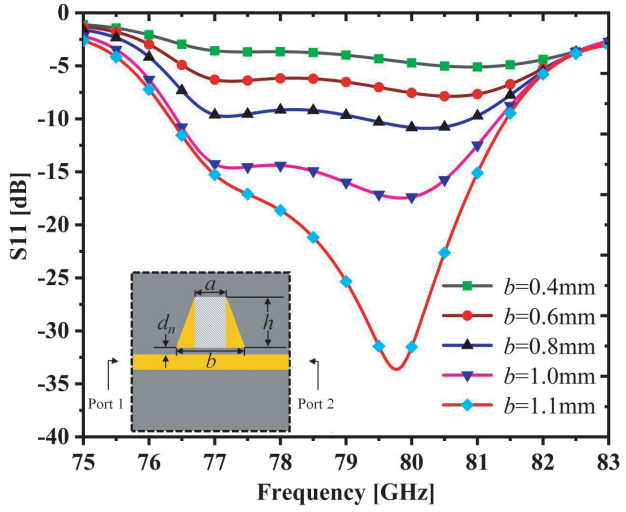

Figure 3. Simulation S_{11} of the proposed linear array with different b.

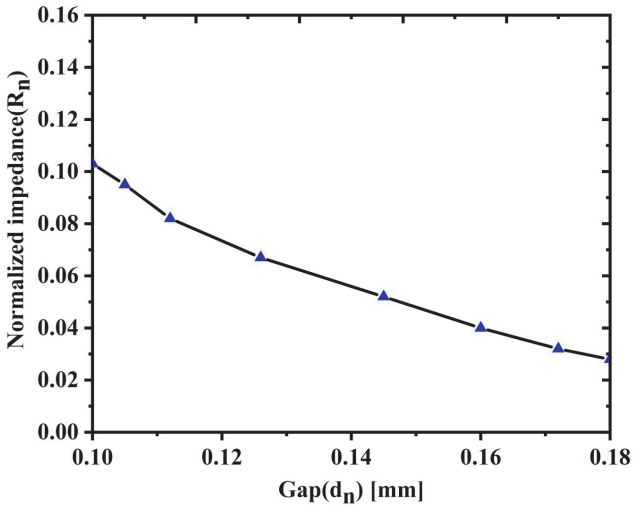

Figure 4. Normalized impedance (R_n) at different gap (d_n).

Similar to [15], it can be deduced that the normalized impedance at the center of the patch R_n is represented by S_{11} as

$$R_n = \frac{Z_n}{Z_0} = \frac{2S_{11}}{1 - S_{11}} \tag{4}$$

As shown in Fig. 4, when the gap d_n increases, the normalized impedance R_n decreases, that is, when the radiating patch is farther away from the feedline, the coupled energy is smaller. The analysis of the impedance characteristics of the unit is of great significance for the array design of low-SLL array antennas.

2.3. Design of Low-SLL Microstrip Linear Arrays

Aiming at the applicability of the proposed proximity coupled microstrip array antenna, a 1×16 linear array antenna is designed, taking the 77–81 GHz frequency band allocated for automotive radar applications as an example.

Figure 1 presents the structure of a 16-element linear array. In antenna design, in order to avoid unnecessary interference from angles outside the region of interest, it is usually necessary to use Taylor-

Table 1. Parameter of the 16-element linear array.

Element Number (n)	Taylor distribution (I_n)	The normalized impedance (R_n)	Gap (d_n, mm)
1, 16	0.52	0.028	0.175
2, 15	0.56	0.032	0.172
3, 14	0.63	0.040	0.160
4, 13	0.71	0.052	0.145
5, 12	0.81	0.067	0.126
6, 11	0.90	0.082	0.112
7, 10	0.96	0.095	0.105
8, 9	1.00	0.103	0.100

distribution to weight the amplitude to suppress SLL. The desired amplitude distribution is determined by the normalized impedance of each trapezoidal radiating element. So a 16-element linear proximity coupled microstrip array antenna with −20 dB low-SLL is designed.

Due to manufacturing tolerances, the minimum gap between the microstrip radiating patch and the center microstrip line is 0.1 mm, and the normalized impedance is the maximum. In addition, after continuous optimization, the gap d_n and normalized impedance of 8 groups of array elements are symmetrically determined to obtain the normalized impedance required to provide −20 dB Taylor-distribution (listed in Table 1). The array was matched to 50 Ω microstrip line by using a 1/4 impedance transformer at the input. The dimension parameters are determined as: $Wf = 0.3$ mm, $a = 0.4$ mm, $b = 1.1$ mm, $h = 1.0$ mm.

3. MEASUREMENT

To verify the proposed array antenna, a prototype of the designed antenna was fabricated, as shown in Fig. 5(a). In order to facilitate the measurement, a broadband microstrip-to-waveguide transition was realized to connect to the WR-10 waveguide [16], and the array antenna reflection performance was measured by a vector network analyzer. Install the antenna on the test platform in an anechoic chamber, and measure the radiation pattern of the antenna in Fig. 5(b).

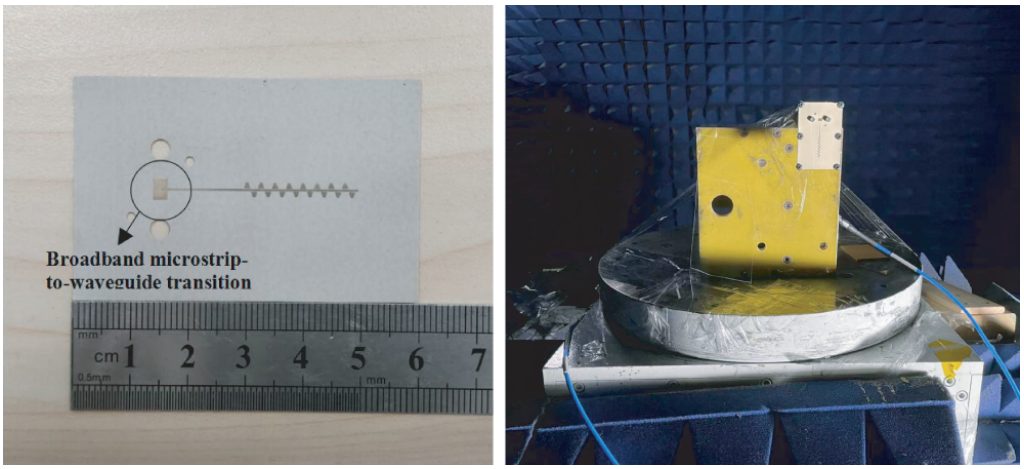

(a) (b)

Figure 5. Photographs: (a) Fabricated 1 × 16 linear array and, (b) measurement setup in an anechoic chamber.

Figure 6 shows the simulated and measured reflection coefficients S_{11} of the proposed antenna around 79 GHz, respectively. In the operating frequency of 77–81 GHz, the measured return loss of 1 × 16 linear is lower than −10 dB, and the measured results are in good agreement with the simulation. Compared with the simulation results, the antennas resonance points are slightly shifted, which is mainly caused by the change of manufacturing tolerances and microstrip-to-waveguide transition structures. The impedance bandwidth of 1×16 proximity coupled microstrip array antenna is 7.6% (75.6–81.6 GHz).

Figure 7 shows the simulated and measured radiation patterns of the proposed antenna at 79, 77, and 81 GHz. It can be seen that the sidelobe level of the E-plane is suppressed below −20 dB. At the design frequency (79 GHz), the measurement results of 1 × 16 linear array verify the performance of the proposed low-SLL antenna, and the half-power beam width is 11°. While the feeder structure seems to increase the SLL, it is still below −20 dB, which is pretty low. At 77, 79, and 81 GHz, the beam direction offset is −1, 0, and +2 degrees, respectively, due to the phase shift caused by frequency change. Because of the proximity coupled structure, this phase shift is very small compared to the traditional series-feed structure. This proves the stability of the proximity coupled structure.

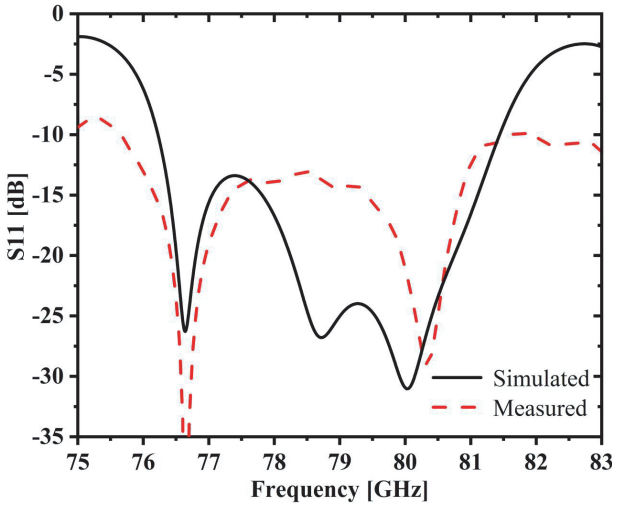

Figure 6. Simulated and measured S_{11} of 1×16 linear array antenna.

Table 2. Comparison of several series-fed linear arrays.

Ref.	No. of Elements	Frequency (GHz)	Impedance bandwidth	Gain (dBi)	No. of layers
[9]	1×26	24.125	3.3%	15.00	Single
[10]	1×8	76.5	3.9%	13.80	Single
[11]	1×8	24.125	1.2%	12.20	Single
[13]	1×7	28	4.6%	14.71	Double
[14]	1×18	79	6.8%	13.94	Single
This work	**1×16**	**79**	**7.6%**	**15.76**	**Single**

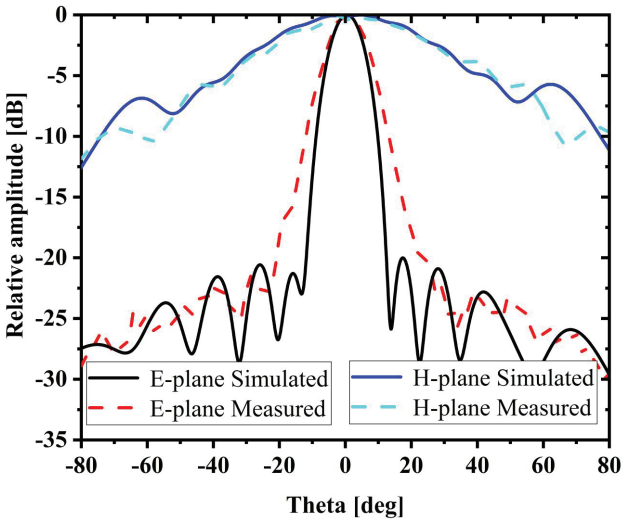

(a)

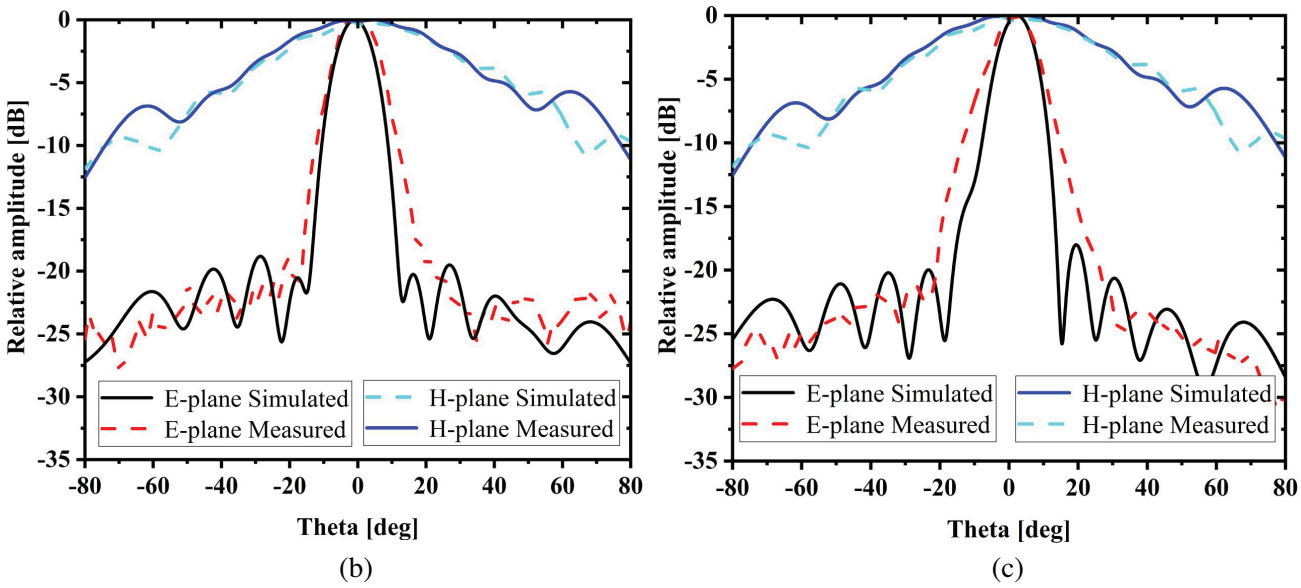

Figure 7. Radiation patterns of 1×16 linear array antenna in the E-plane and H-plane at (a) 79 GHz, (b) 77 GHz, (c) 81 GHz.

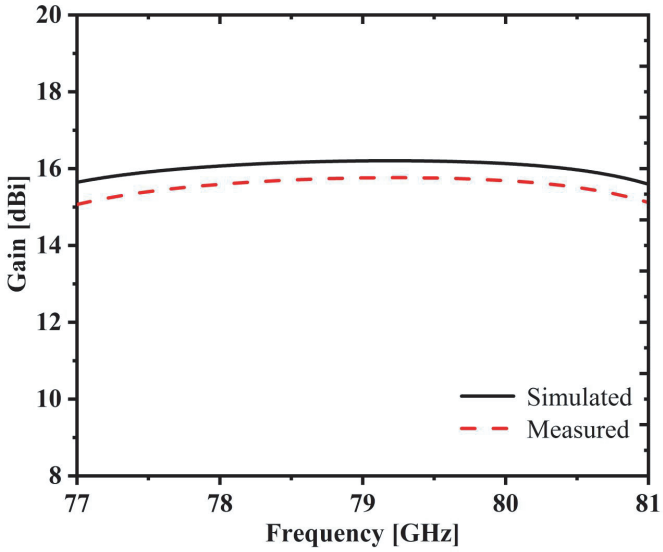

Figure 8. Gain of 1×16 linear array antenna.

Figure 8 shows the simulated and measured gain plots of the proposed antenna. For the operating frequency range of 77–81 GHz, the measured gain of linear array is higher than 15 dBi and is stable within a 1 dBi variation range. The difference between the measured and simulated gains is about 1 dBi, mainly due to the presence of the transition structure.

Table 2 shows the performance comparison between the proposed 1×16 linear array and several reported series-fed linear arrays. The proposed proximity-coupled linear array can achieve a wider impedance bandwidth and higher gain than previous works. The proposed linear array has a compact structure and uses a single-layer dielectric plate, which is very suitable for radar sensor applications.

4. CONCLUSIONS

A broadband proximity coupled millimeter-wave microstrip array antenna for automotive radar applications is proposed. In the design of the array antenna, the broadband characteristic is achieved by adopting the proximity coupling feeding method, and the structure adjusts the gap between the trapezoidal radiating element and the feedline to control the normalized resistance, so that it is easy to achieve low SLL. The introduction of the trapezoidal patch enhances the excitation coupling while suppressing out-of-band frequencies, and it has a wider impedance bandwidth than a rectangular patch. In order to verify the feasibility of the design, a 1×16 linear array covering the 77–81 GHz frequency band is designed for automotive radar applications. The simulated low SLL and bandwidth characteristics of the array antenna are in good agreement with the measured results, and the stable gain in the working bandwidth is also obtained.

ACKNOWLEDGMENT

This work was supported in part by the Postgraduate Research & Practice Innovation Program of Jiangsu Province (No. KYCX21_0877), and in part by the Jiangsu Agriculture Science and Technology Innovation Fund (JASTIF; Project number: CX(21)3187).

REFERENCES

1. Schram, R., A. Williams, and M. van Ratingen, "Implementation of Autonomous Emergency Braking (AEB), the next step in euro NCAP's safety assessment," *2013 Proc. of the Int. Technical Conf. Onthe Enhanced Safety of Vehicles (ESV)*, Seoul, Republic of Korea, May 27–30, 2013.
2. Weiss, M., "Microstrip antennas for millimeter waves," *IEEE Trans. Antennas Propag.*, Vol. 29, No. 1, 171–174, January 1981.
3. Xu, J., W. Hong, H. Zhang, G. Wang, Y. Yu, and Z. H. Jiang, "An array antenna for both long- and medium-range 77 GHz automotive radar applications," *IEEE Trans. Antennas Propag.*, Vol. 65, No. 12, 7207–7216, December 2017.
4. Yu, Y., W. Hong, Z. H. Jiang, and H. Zhang, "E-band low-profile, wideband 45° linearly polarized slot-loaded patch and its array for millimeter-wave communications," *IEEE Trans. Antennas Propag.*, Vol. 66, No. 8, 4364–4369, August 2018.
5. Li, M. and K. Luk, "Low-cost wideband microstrip antenna array for 60-GHz applications," *IEEE Trans. Antennas Propag.*, Vol. 62, No. 6, 3012–3018, June 2014.
6. Guo, Y. Q., Y. M. Pan, and S. Y. Zheng, "Design of series-fed, single-layer, and wideband millimeter-wave microstrip arrays," *IEEE Trans. Antennas Propag.*, Vol. 68, No. 10, 7017–7026, October 2020.
7. Xu, H., J. Zhou, K. Zhou, Q. Wu, Z. Yu, and W. Hong, "Planar wideband circularly polarized cavity-backed stacked patch antenna array for millimeter-wave applications," *IEEE Trans. Antennas Propag.*, Vol. 66, No. 10, 5170–5179, October 2018.
8. Yuan, T., N. Yuan, and L. Li, "A novel series-fed taper antenna array design," *IEEE Antennas Wireless Propag. Lett.*, Vol. 7, 362–365, 2008.
9. Khalili, H., K. Mohammadpour-Aghdam, S. Alamdar, and M. Mohammad-Taheri, "Low-cost series-fed microstrip antenna arrays with extremely low sidelobe levels," *IEEE Trans. Antennas Propag.*, Vol. 66, No. 9, 4606–4612, September 2018.
10. Kang, Y., E. Noh, and K. Kim, "Design of traveling-wave series-fed microstrip array with a low sidelobe level," *IEEE Antennas Wireless Propag. Lett.*, Vol. 19, No. 8, 1395–1399, August 2020.
11. Qian, J., H. Zhu, M. Tang, and J. Mao, "A 24 GHz microstrip comb array antenna with high sidelobe suppression for radar sensor," *IEEE Antennas Wireless Propag. Lett.*, Vol. 20, No. 7, 1220–1224, July 2021.

12. Diawuo, H. A. and Y.-B. Jung, "Broadband proximity-coupled microstrip planar antenna array for 5G cellular applications," *IEEE Antennas Wireless Propag. Lett.*, Vol. 17, No. 7, 1286–1290, July 2018.
13. Dzagbletey, P. A. and Y.-B. Jung, "Stacked microstrip linear array for millimeter-wave 5G baseband communication," *IEEE Antennas Wireless Propag. Lett.*, Vol. 17, No. 5, 780–783, May 2018.
14. Lee, J.-H., J. M. Lee, K. C. Hwang, D.-W. Seo, D. Shin, and C. Lee, "Capacitively coupled microstrip comb-line array antennas for millimeter-wave applications," *IEEE Antennas Wireless Propag. Lett.*, Vol. 19, No. 8, 1336–1339, August 2020.
15. Liu, D., H. Nakano, X. Qing, and T. Zwick, *Handbook of Antenna Technologies*, 1389–1413, Springer, Gateway East, Singapore, 2016.
16. Seo, K., "Planar microstrip-to-waveguide transition in millimeter-wave band," *Advancement in Microstrip Antennas with Recent Applications*, Ch. 11, 249–277, A. Kishk, Ed., InTech, Rijeka, Croatia, 2013.